Electronic Supplementary Information

Contactless acoustic tweezer for droplet manipulation on superhydrophobic surfaces

Tao Luo[a,b]*, Sirui Liu[a], Rui Zhou[a], Chen Zhang[a], Dongyang Chen[a], Yi Zhan[c], Qilin Hu[d], Xi He[d], Yu Xie[a], Zhijie Huan[e], Wendi Gao[f], Ruirui Li[g], Gongfa Yuan[a], Yancheng Wang[b] and Wei Zhou[a]*

[a] Pen-Tung Sah Institute of Micro-Nano Science and Technology, Xiamen University, Xiamen, 361102, China.;
[b] The State Key Laboratory of Fluid Power & Mechatronic Systems, Zhejiang University, Hangzhou 310027, China;
[c] AECC Gui Zhou Liyang Aviation Power Co., Ltd. Guiyang, 550014, China;
[d] School of Aerospace Engineering, Xiamen University, Xiamen, 361102, China;
[e] School of Electrical Engineering and Automation, Xiamen University of Technology, Xiamen, 361024, China;
[f] The State Key Laboratory for Manufacturing Systems Engineering, International Joint Laboratory for Micro/Nano Manufacturing and Measurement Technologies, Overseas Expertise Introduction Center for Micro/Nano Manufacturing and Nano Measurement Technologies Discipline Innovation, Xi'an Jiaotong University, Xi'an 710049, China.
[g] *State Key Laboratory of Dynamic Measurement Technology, North University of China, Taiyuan, 030051, P.R. China.*

* Corresponding authors: Tao Luo and Wei Zhou

Email: luotao@xmu.edu.cn; weizhou@xmu.edu.cn;

This file includes:

Other supplementary materials for this manuscript include the following:

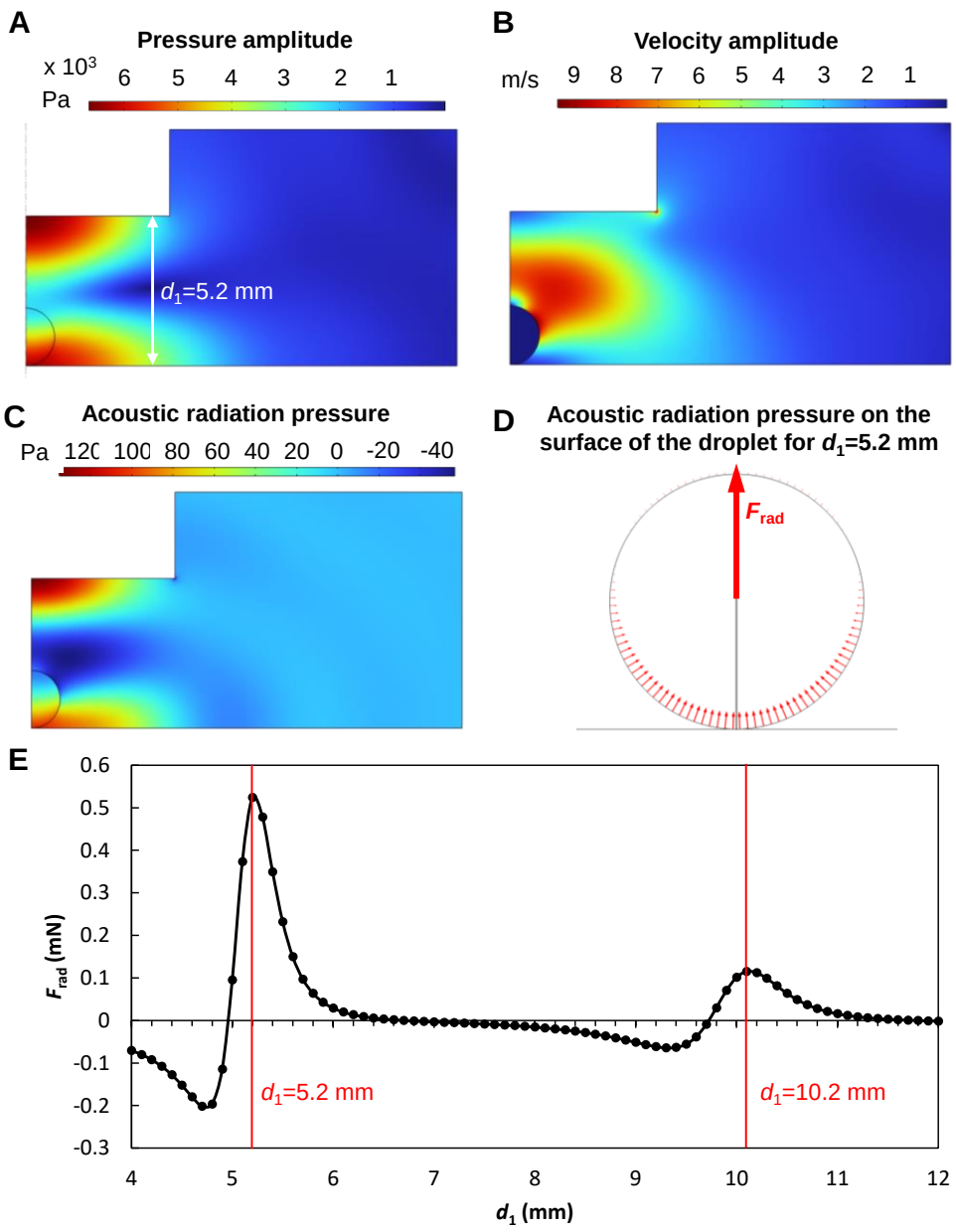

Fig. S1 Numerical simulation of droplet levitation with the CAT. The droplet has a radius of 1 mm and is positioned 5.2 mm away from the reflector. (A) Amplitude of acoustic pressure. (B) Amplitude of acoustic medium particle velocity. (C) Distribution of acoustic radiation pressure. (D) Acoustic radiation pressure acting on droplet surface, resulting in upward acoustic radiation force $\boldsymbol{F}_{\mathbf{rad}}$ for levitation. (E) Acoustic radiation force $\boldsymbol{F}_{\mathbf{rad}}$ versus distance d_1, with positive values representing upward force and negative values representing downward force. Droplet levitation can easily occur at two different distances (d_1=5.2 and 10.2 mm) between the UST and reflector, which are close to λ/2 and λ, respectively.

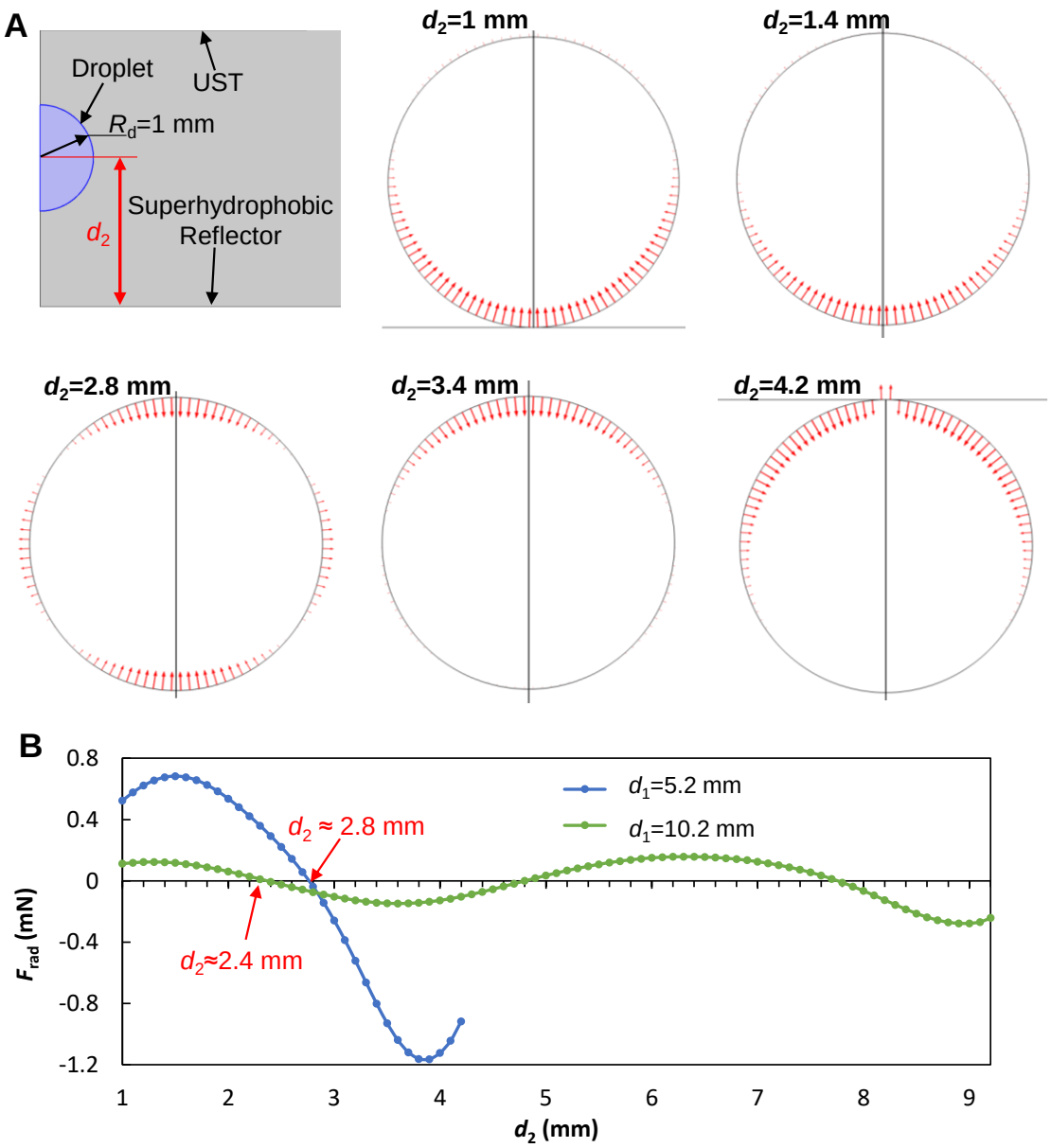

Fig. S2 Influence of droplet position and radius on the acoustic radiation force F_{rad}. (A) Acoustic radiation pressure on droplet surface at different vertical positions (d_2) when the distance (d_1) between the droplet and the reflector is fixed at 5.2 mm. (B) The acoustic radiation force F_{rad} versus the vertical position (d_2) of the droplet at two different distances (d_1=5.2 and 10.2 mm) between the UST and the reflector. The droplet will be levitated and balanced at heights of 2.4 and 2.8 mm accordingly, where the acoustic radiation force F_{rad} become zero.

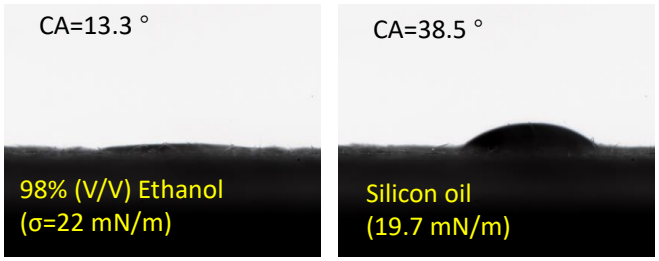

Fig. S3 Contact angles of 8 µL 98% (V/V) ethanol and silicon oil on the superhydrophobic paper.

Various liquids with different surface tensions (ranging from 25 to 72 mN/m) were prepared based on data available in the Ref [1–3]. Surface tensions ranging from 22 to 30 mN/m were obtained by mixing ethanol with DI water in different volume ratios, and adjusting the ratio of TWEEN 20 in DI water obtained liquids with surface tensions ranging from 38 to 72 mN/m. Silicon oil has the lowest surface tension of 19.7 mN/m.

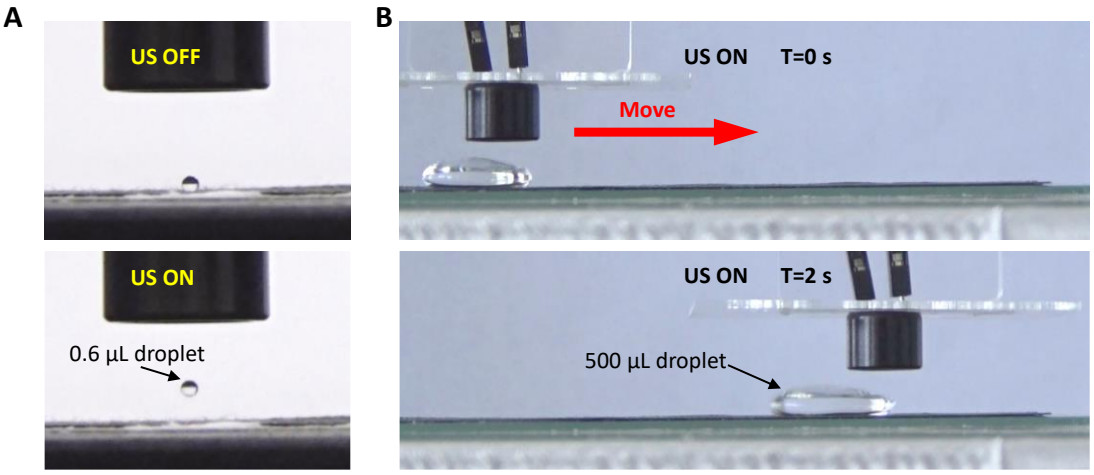

Fig. S4 Upper and lower limits of droplet volume that can be manipulated by the proposed acoustic tweezers. (A) Levitation of a 0.6 µL droplet. (B) In-plane manipulation of a 500 µL droplet.

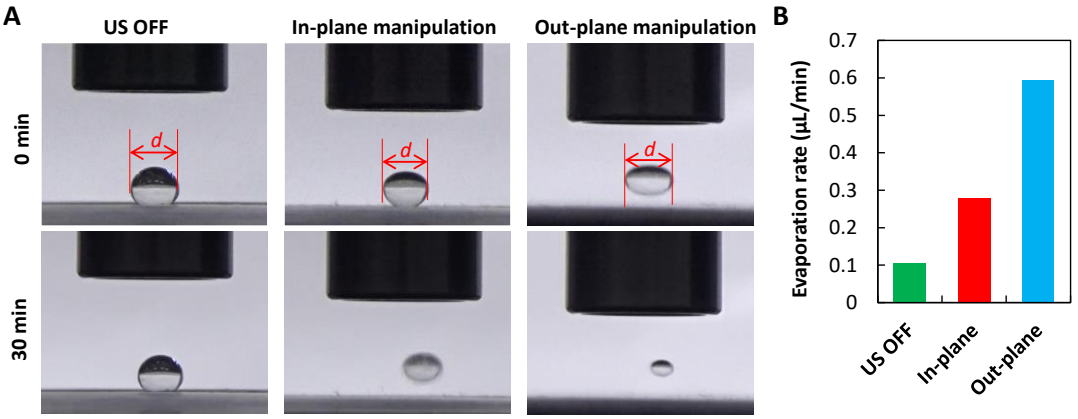

Fig. S5 Evaporation of three 20 µL droplets. (A) Images depicting the size variation of three droplets before and after a 30-minute evaporation process under three different conditions: natural evaporation without ultrasound, evaporation with in-plane manipulation using the proposed CAT, and evaporation with out-plane manipulation using the proposed CAT. (B) Evaporation rates of droplets under three different conditions. The evaporation rate in volume is estimated based on the length variation of the major axis (d) of ellipse-shaped droplets. As the volume of a droplet V is proportional to d^3, hence the evaporation rate of a 20 µL droplet can be approximated as $V_0 \cdot (1 - (d_{30}/d_0)^3)/30$, where V_0 is the initial volume of the droplet, d_{30} is the length of the major axis of the droplet after 30 minutes of evaporation, and d_0 is length of the major axis of the droplet in its initial state.

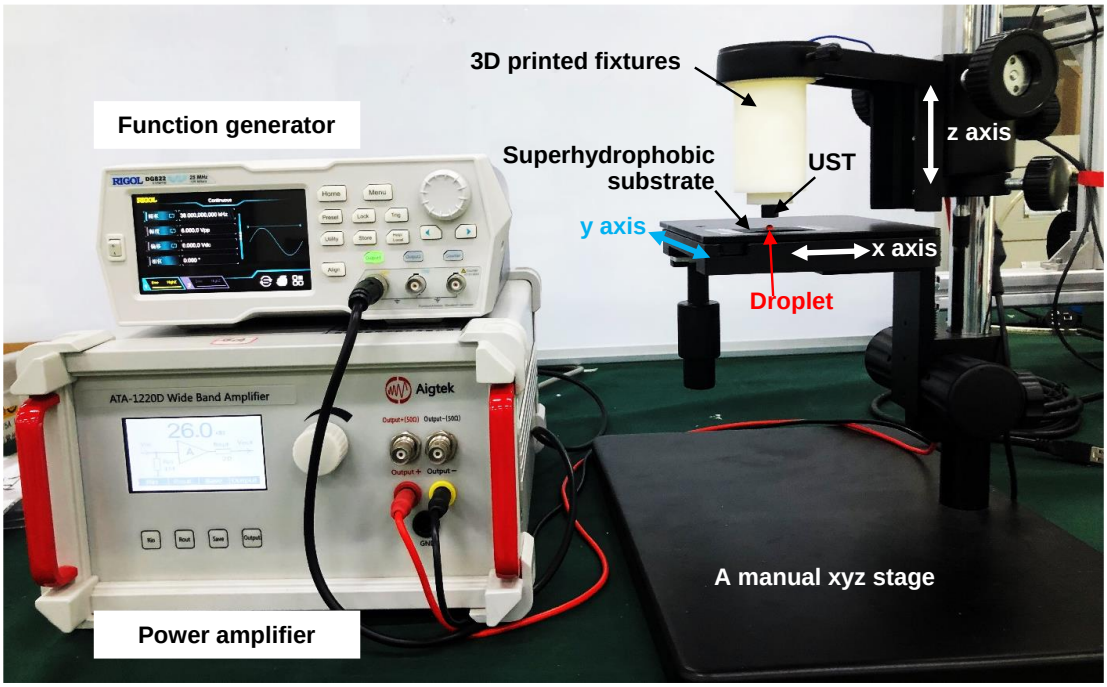

Fig. S6 The custom-made hardware setup for the CAT.

Supplementary Movies

Movie S1 (separate file). High speed imaging shows the dynamic process for levitating a 10 µL droplet from the superhydrophobic surface by using the proposed contactless acoustic tweezer (CAT).

Movie S2 (separate file). Acoustic levitation of a 10 µL droplet from six substrates with different contact angles and sliding angles.

Movie S3 (separate file). Acoustic levitation of a 10 µL droplet from superhydrophobic copper, Polymethyl methacrylate, and glass substrates.

Movie S4 (separate file). Out-plane manipulation of 20 µL aqueous droplets with different surface tensions.

Movie S5 (separate file). Levitating droplets with different volumes from the superhydrophobic surface by using the CAT.

Movie S6 (separate file). Contactless transportation trials of a 50 µL droplet on six substrates with different contact angles and sliding angles.

Movie S7 (separate file). In-plane manipulation of 20 µL aqueous droplets with different surface tensions.

Movie S8 (separate file). Contactless transportation of a 3 and 200 µL droplet on the same superhydrophobic paper by using the CAT with same operation conditions.

Movie S9 (separate file). Maximum movement velocities of the ultrasonic transducer for droplets with different volumes to follow.

Movie S10 (separate file). Contactless transportation of 20 µL red-color water, soy milk and coke droplets on the same superhydrophobic paper.

Movie S11 (separate file). Merge two droplets with the CAT enhances the mixing rate compared with the coalescence of two droplets by a pipette tip.

Movie S12 (separate file). The CAT based continuous transportation and merging of five 20 µL water droplets with different colors.

Movie S13 (separate file). The CAT based sequential coalescence of three droplets with vinegar, litmus, and sodium carbonate.

Movie S14 (separate file). Evaporation of three 20 µL droplets under three different conditions: natural evaporation without ultrasound, evaporation with in-plane manipulation using the proposed CAT, and evaporation with out-plane manipulation using the proposed CAT.

References

1 N. Rehman, H. Ullah, S. Alam, A. K. Jan, S. W. Khan and M. Tariq, *J. Mater. Environ. Sci.*, 2017, **8**, 1161–1167.

2 M. Sharma, P. K. Roy, J. Barman and K. Khare, *Langmuir*, 2019, **35**, 7672–7679.

3 M. J. Owen and J. L. Groh, *J. Appl. Polym. Sci.*, 1990, **40**, 789–797.